Transient Response of a Permeable Crack Normal to a Piezoelectric-elastic Interface : Anti-plane Problem

Soon Man Kwon
Department of Mechanical Design & Manufacturing, Changwon National University, 9 Sarim-dong, Changwon, Kyongnam 641-773, Korea
Kang Yong Lee*
School of Mechanical Engineering, Yonsei University, Seoul 120-749, Korea

In this paper, the anti-plane transient response of a central crack normal to the interface between a piezoelectric ceramics and two same elastic materials is considered. The assumed crack surfaces are permeable. By virtue of integral transform methods, the electroelastic mixed boundary problems are formulated as two set of dual integral equations, which, in turn, are reduced to a Fredholm integral equation of the second kind in the Laplace transform domain. Time domain solutions are obtained by inverting Laplace domain solutions using a numerical scheme. Numerical values on the quasi-static stress intensity factor and the dynamic energy release rate are presented to show the dependences upon the geometry, material combination, electromechanical coupling coefficient and electric field.

Key Words: Anti-Plane Shear Impact, Piezoelectric-Elastic Composites, Permeable Crack, Intensity Factors, Electromechanical Coupling Coefficient

1. Introduction

Piezoelectric materials generate an electric field when subjected to strain fields and undergo deformation when an electric field is applied. This inherent electromechanical coupling is widely exploited in the design of many devices like transducers, sensors and actuators. In addition, piezoelectric materials are a primary concern in the field of advanced lightweight structures where the smart structure technology is now emerging (Crawley, 1994). By bonding or merging piezoelectric members within a structure it is possible to control the structure behavior through electrically induced strain fields and, conversely, employ the strain-induced electric field as a feedback driver. The effective control of piezoelectric smart structures can be achieved by means of the optimal combination of structural and control elements, which allows using all the benefits of the electromechanical coupling. On the while, due to the brittle behavior of piezoelectric materials, reliable service lifetime predictions demand a comprehensive understanding of the fracture process in the presence of electromechanical coupling. In many engineering applications, these piezoelectric structures may experience transient dynamic loads as well as steady harmonic loads. It is, therefore, of great importance to investigate the transient dynamic response of cracked piezoelectric structures.

A finite crack in an infinite piezoelectric material under anti-plane electromechanical impact was investigated by Chen and coworkers (Chen and Yu, 1997 ; Chen and Karihaloo, 1999) with an impermeable crack boundary condition. The same problem of an anti-plane shear wave in an infinite piezoelectric medium were considered by Chen and Yu (1998) with the impermeable

* Corresponding Author,
E-mail : KYL2813@yahoo.co.kr
TEL : +82-2-2123-2813; **FAX** : +82-2-2123-2813
School of Mechanical Engineering, Yonsei University, Seoul 120-749, Korea. (Manuscript **Received** June 17, 2003; **Revised** June 3, 2004)

crack boundary condition, and Meguid and Wang (1998) with the permeable one, respectively. The impermeable and the permeable results for an infinite piezoelectric strip parallel to the crack under anti-plane shear impact loading were reported by Chen (1998) and Li and Fan (2002), respectively. Shin et al.(2001) presented an eccentric permeable crack solution in an infinite piezoelectric strip parallel to the crack under anti-plane shear impact loading. Chen and Meguid (2000) studied a vertical crack problem in an infinite piezoelectric strip under anti-plane electromechanical impact load based on impermeable crack model. Kwon and Lee (2001) presented transient dynamic solutions for a rectangular shaped piezoelectric material with both the permeable and the impermeable crack condition. Most recently, Kwon and Lee (2004) considered the dynamic response of an anti-plane crack on the basis of the unified crack boundary condition in a functionally graded piezoelectric strip.

The appropriate choice of electrical boundary conditions on the crack surface is still an open problem. Generally, there are two well-accepted electric boundary conditions, namely; the permeable and impermeable ones. An impermeable boundary condition on the crack surface has been widely used in the previous works. Although this assumption can simplify some analysis and is shown to be valid to the problem of a nonslender hole, however, it may lead to erroneous results for crack problems. Particularly, since no opening displacement exists for an anti-plane problem, the crack surfaces can be in perfect contact. Therefore, the classical electric boundary conditions along the interface of dielectric materials (the continuity of the normal component of electric displacement and tangential component of electric field), i.e. permeable crack model, are considered in the current study.

In this paper, we consider the problem for a crack in a rectangular shaped piezoelectric block bonded between two same elastic blocks under the combined anti-plane mechanical shear and in-plane electrical transient loadings. By using integral transform techniques, the problem is reduced to a Fredholm integral equation of the second kind in the Laplace transform domain, which are obtained from two pairs of dual integral equations. Time domain solutions are obtained by inverting Laplace domain solutions using a numerical scheme. Though main purpose of the present work is to seek the transient dynamic solution for a piezoelectric-elastic composite structure with classic electric boundary conditions, the quasi-static result is also discussed in detail since the recent work (Kwon and Meguid, 2002) misleads the readers. Numerical results of the quasi-static stress intensity factor and the dynamic energy release rate are also displayed graphically to show the dependences upon the geometry, material combination, electromechanical coupling coefficient and electric field.

2. Formulation of the Problem

Consider the problem of a piezoelectric composite block of height $2h$ and width $2b_0$, which consists of the piezoelectric and elastic materials. A central through crack of length $2a$ is located in the mid-plane of the piezoelectric block and the crack boundaries are parallel to the -axis, as shown in Fig. 1. Here Cartesian coordinates (x, y, z) are the principal axes of the material symmetry while the z-axis is oriented in the poling direction of the piezoelectric block. Anti-plane mechanical loading and in-plane electric

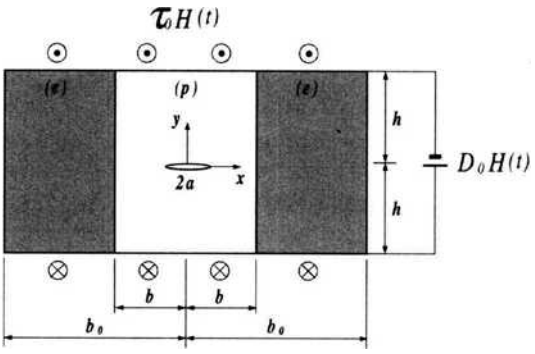

Fig. 1 Piezoelectric-elastic composite block with a center crack (e): elastic material, (p): piezoelectric material

loading are suddenly exerted on the top and bottom surfaces of the composite block. τ_0, D_0 and $H(t)$ in Fig. 1 refer to the applied shear traction, the electric displacement and the Heaviside unit step function, respectively.

The dynamic anti-plane electroelastic governing equations in the absence of body forces and free charge can be written by the following forms,

$$\nabla^2 w=\frac{1}{C_T^2}\frac{\partial^2 w}{\partial t^2} \tag{1}$$

$$\nabla^2 w_e=\frac{1}{C_{Te}^2}\frac{\partial^2 w_e}{\partial t^2} \tag{2}$$

$$\nabla^2 \psi_i=0 \tag{3}$$

where $w(x, y, t)$, $w_e(x, y, t)$ and $\psi(x, y, t)$ are the mechanical displacements of the piezoelectric-elastic composite bock and the Bleustein function (Bleustein, 1968), respectively. Quantities in two elastic blocks will subsequently be designated by subscripts e. And $\nabla^2=\partial^2/\partial x^2+\partial^2/\partial y^2$ represents the two-dimensional Laplacian operator. Also

$$\begin{gathered} C_T=\sqrt{\frac{\mu}{\rho}};\ C_{Te}=\sqrt{\frac{c_{44e}}{\rho_e}};\\ \mu=c_{44}+\frac{e_{15}^2}{d_{11}};\ \psi=\phi-\frac{e_{15}}{d_{11}}w \end{gathered} \tag{4}$$

in which C_T, C_{Te}, μ, c_{44e}, ρ and ρ_e are the speed of the piezoelectrically stiffened bulk shear wave, the speed of the shear wave in elastic layers, the piezoelectrically stiffened elastic constant, the elastic shear modulus of the elastic material, the piezoelectric material density, and the elastic material density, respectively. In addition to the above coefficients, c_{44}, d_{11}, e_{15} and ϕ are the elastic shear modulus measured in a constant electric field, the dielectric permittivity measured at a constant strain, the piezoelectric constant, and the electric potential, respectively.

Once functions w, w_e and ψ are determined from given boundary conditions, then the components of anti-plane shear stress, in-plane electric displacement, D_x, D_y, and electric field, E_x, E_y, are obtainable in terms of the following constitutive relations:

$$\tau_{kz}=\mu w,_k+e_{15}\psi,_k,\ \tau_{kze}=c_{44e}w_e,_k \tag{5}$$

$$D_k=-d_{11}\psi,_k,\ E_k=-\phi,_k \tag{6}$$

where comma denotes partial differentiation with respect to $k(k=x, y)$.

Owing to the symmetry in geometry and loading, in the following, it is sufficient to consider only the quarter-plane. As usual, the problem can be separated into two subproblems and solved by superposition. From the viewpoint of fracture mechanics, or practical interest is the dynamic singular electroelastic field due to the presence of the crack. Consequently, in what follows we focus our attention on the perturbation solution for a crack. Considering the geometry and electromechanical loading, the electroelastic boundary conditions could be satisfied as follows:

$$D_x(b, y, t)=0,\ (0\le y\le h) \tag{7}$$

$$w(b, y, t)=w_e(b, y, t),\ (0\le y\le h) \tag{8}$$

$$\tau_{xz}(b, y, t)=\tau_{xze}(b, y, t),\ (0\le y\le h) \tag{9}$$

$$\tau_{yz}(x, 0, t)=-\tau_0 H(t),\ (0\le x<a) \tag{10}$$

$$w(x, 0, t)=0,\ (a<x\le b) \tag{11}$$

$$D_y(x, 0^+, t)=D_y(x, 0^-, t),\ (0\le x<a) \tag{12a}$$

$$E_x(x, 0^+, t)=E_x(x, 0^-, t),\ (0\le x<a) \tag{12b}$$

$$\phi(x, 0, t)=0,\ (a<x\le b) \tag{13}$$

3. Solution to the Problem

In order to obtain the singular electroelastic field, it is necessary to assume that the composed materials are static at the initial time. Under such circumstances, it is easily shown from Eqs. (1)~(3) that the out-of-plane displacements $w(x, y, t)$, $w_e(x, y, t)$ and the Bleustein function $\psi(x, y, t)$ in the Laplace transform domain with respect to time can take the forms (Kwon and Lee; 2000, 2001):

$$w^*(x, y, p) = \frac{2}{\pi}\int_0^\infty A_1(s, p)\frac{\cosh[\gamma(h-y)]}{\cosh(\gamma h)}\cos(sx)\,ds + \sum_{n=0}^{\infty} B_1(n, p)\cosh(\lambda x)\sin(\beta y/h) \tag{14}$$

$$\phi^*(x, y, p) = \frac{2}{\pi}\int_0^\infty A_2(s, p)\frac{\cosh[s(h-y)]}{\cosh(sh)}\cos(sx)\,ds + \sum_{n=0}^{\infty} B_2(n, p)\cosh(\beta x/h)\sin(\beta y/h) \tag{15}$$

$$w_e^*(x, y, p) = \sum_{n=0}^{\infty} C(n, p)\cosh[\lambda_e(b_0-x)]\sin(\beta y/h) \tag{16}$$

where

$$\gamma=\sqrt{s^2+(p/C_T)^2},\quad \beta=(2n+1)\pi/2$$
$$\lambda=\sqrt{(\beta/h)^2+(p/C_T)^2} \tag{17}$$
$$\lambda_e=\sqrt{(\beta/h)^2+(p/C_{Te})^2}$$

$A_j(s, p)$, $B_j(n, p)$ $(j=1, 2)$ and $C(n, p)$ are the unknown functions to be determined from the given boundary conditions. Superscript $*$ and p denote Laplace transform domain and Laplace transform parameter, respectively, defined by

$$f^*(p) = \int_0^\infty f(t)\,e^{-pt}dt \tag{18}$$

$$f(t) = \frac{1}{2\pi i}\int_{Br} f^*(p)\,e^{pt}dp \tag{19}$$

where the integral in Eq. (19) is taken over the Bromwich path.

Furthermore, it follows from last relation of Eq. (4) that the electric potential $\phi(x, y, t)$ in the Laplace transform domain is given by

$$\phi^*(x, y, p) = \frac{2}{\pi}\frac{e_{15}}{d_{11}}\int_0^\infty A_1(s, p)\frac{\cosh[\gamma(h-y)]}{\cosh(\gamma h)}\cos(sx)\,ds + \frac{e_{15}}{d_{11}}\sum_{n=0}^{\infty} B_1(n, p)\cosh(\lambda x)\sin(\beta y/h) + \frac{2}{\pi}\int_0^\infty A_2(s, p)\frac{\cosh[s(h-y)]}{\cosh(sh)}\cos(sx)\,ds + \sum_{n=0}^{\infty} B_2(n, p)\cosh(\beta x/h)\sin(\beta y/h) \tag{20}$$

With the aid of constitutive equations, from Eqs. (5) and (6) it is not difficult to obtain the expressions for the components of the stress, strain, electric displacement and the electric field in the Laplace transform domain in terms of $A_j(s, p)$, $B_j(n, p)$ and $C(n, p)$, $j=1, 2$. For instance, we have :

$$\tau_{xz}^*(x, y, p) = -\frac{2\mu}{\pi}\int_0^\infty sA_1(s, p)\frac{\cosh[\gamma(h-y)]}{\cosh(\gamma h)}\sin(sx)\,ds + \mu\sum_{n=0}^{\infty}\lambda B_1(n, p)\sinh(\lambda x)\sin(\beta y/h) - \frac{2e_{15}}{\pi}\int_0^\infty sA_2(s, p)\frac{\cosh[s(h-y)]}{\cosh(sh)}\sin(sx)\,ds + e_{15}\sum_{n=0}^{\infty}\frac{\beta}{h}B_2(n, p)\sinh(\beta x/h)\sin(\beta y/h) \tag{21}$$

$$\tau_{yz}^*(x, y, p) = -\frac{2\mu}{\pi}\int_0^\infty \gamma A_1(s, p)\frac{\sinh[\gamma(h-y)]}{\cosh(\gamma h)}\cos(sx)\,ds + \mu\sum_{n=0}^{\infty}\frac{\beta}{h}B_1(n, p)\cosh(\lambda x)\cos(\beta y/h) - \frac{2e_{15}}{\pi}\int_0^\infty sA_2(s, p)\frac{\sinh[s(h-y)]}{\cosh(sh)}\cos(sx)\,ds + e_{15}\sum_{n=0}^{\infty}\frac{\beta}{h}B_2(n, p)\cosh(\beta x/h)\cos(\beta y/h) \tag{22}$$

$$\tau_{xze}^*(x, y, p) = -c_{44e}\sum_{n=0}^{\infty}\lambda_e C(n, p)\sinh[\lambda_e(b_0-x)]\sin(\beta y/h) \tag{23}$$

$$\tau_{yze}^*(x, y, p) = c_{44e}\sum_{n=0}^{\infty}\frac{\beta}{h}C(n, p)\cosh[\lambda_e(b_0-x)]\cos(\beta y/h) \tag{24}$$

$$D_x^*(x, y, p) = \frac{2d_{11}}{\pi}\int_0^\infty sA_2(s, p)\frac{\cosh[s(h-y)]}{\cosh(sh)}\sin(sx)\,ds - d_{11}\sum_{n=0}^{\infty}\frac{\beta}{h}B_2(n, p)\sinh(\beta x/h)\sin(\beta y/h) \tag{25}$$

$$D_y^*(x, y, p) = \frac{2d_{11}}{\pi}\int_0^\infty sA_2(s, p)\frac{\sinh[s(h-y)]}{\cosh(sh)}\cos(sx)\,ds - d_{11}\sum_{n=0}^{\infty}\frac{\beta}{h}B_2(n, p)\cosh(\beta x/h)\cos(\beta y/h) \tag{26}$$

$$E_x^*(x, y, p)$$
$$=\frac{2}{\pi}\frac{e_{15}}{d_{11}}\int_0^\infty sA_1(s, p)\frac{\cosh[\gamma(h-y)]}{\cosh(\gamma h)}\cos(sx)\,ds$$
$$-\frac{e_{15}}{d_{11}}\sum_{n=0}^{\infty}\lambda B_1(n, p)\sinh(\lambda x)\sin(\beta y/h)$$
$$+\frac{2}{\pi}\int_0^\infty sA_2(s, p)\frac{\cosh[s(h-y)]}{\cosh(sh)}\sin(sx)\,ds \quad (27)$$
$$-\sum_{n=0}^{\infty}\frac{\beta}{h}B_2(n, p)\sinh(\beta x/h)\sin(\beta y/h)$$

$$E_y^*(x, y, p)$$
$$=\frac{2}{\pi}\frac{e_{15}}{d_{11}}\int_0^\infty \gamma A_1(s, p)\frac{\sinh[\gamma(h-y)]}{\cosh(\gamma h)}\cos(sx)\,ds$$
$$-\frac{e_{15}}{d_{11}}\sum_{n=0}^{\infty}\frac{\beta}{h}B_1(n, p)\cosh(\lambda x)\cos(\beta y/h)$$
$$+\frac{2}{\pi}\int_0^\infty sA_2(s, p)\frac{\sinh[s(h-y)]}{\cosh(sh)}\cos(sx)\,ds \quad (28)$$
$$-\sum_{n=0}^{\infty}\frac{\beta}{h}B_2(n, p)\cosh(\beta x/h)\cos(\beta y/h)$$

It can be easily shown that Eq. (16) is satisfied with the conditions of $\tau_{xze}(b_0, y, t)=0$, $(0\le y\le h)$ and $w_e(x, 0, t)=0$, $(b\le x\le b_0)$.

Using the Fourier sine and cosine series pairs, Eqs. (7) ~ (9) yield the following relations

$$B_1(n, p)$$
$$=\frac{4(\beta/h)^2}{\pi\beta c_{44e}r(n, p)}\int_0^\infty\frac{[s\mu\sin(sb)-c_{44e}q\cos(sb)]}{s^2+\lambda^2}A_1(s, p)\,ds \quad (29)$$

$$B_2(n, p)$$
$$=\frac{4}{\pi h\sinh(\beta b/h)}\int_0^\infty\frac{s\cdot\sin(sb)}{s^2+(\beta/h)^2}A_2(s, p)\,ds \quad (30)$$

$$C(n, p)$$
$$=\frac{1}{\cosh[\lambda_e(b-b_0)]}\left\{B_1(n, p)\cosh(\lambda b)\right.$$
$$\left.+\frac{4(\beta/h)^2}{\pi\beta}\int_0^\infty\frac{\cos(sb)A_1(s, p)}{\gamma^2+(\beta/h)^2}ds\right\} \quad (31)$$

where

$$r(n, p)=\frac{\mu}{c_{44e}}\lambda\sinh(\lambda b)+q\cosh(\lambda b) \quad (32)$$

$$q=\lambda_e\tanh[\lambda_e(b_0-b)] \quad (33)$$

In the case of permeable crack surface condition, the following two pairs of dual integral equations are obtained from Eqs. (10) ~ (13):

$$-\frac{2}{\pi}\int_0^\infty s\left[\frac{\mu\gamma\tanh(\gamma h)}{s}A_1(s, p)+e_{15}\tanh(sh)A_2(s, p)\right]\cos(sx)\,ds$$
$$+\mu\sum_{n=0}^{\infty}\frac{4(\beta/h)^2\cosh(\lambda x)}{\pi h c_{44e}r(n, p)}\int_0^\infty\frac{[s\mu\sin(sb)-c_{44e}q\cos(sb)]}{s^2+\lambda^2}A_1(s, p)\,ds \quad (34)$$
$$+e_{15}\sum_{n=0}^{\infty}\frac{4(\beta/h)}{\pi h\sinh(\beta b/h)}\cosh(\beta x/h)\int_0^\infty\frac{s\cdot\sin(sb)A_2(s, p)}{s^2+(\beta/h)^2}ds=-\frac{\tau_0}{p},$$
$$0\le x<a$$

$$\int_0^\infty A_1(s, p)\cos(sx)\,ds=0,\quad a<x\le b \quad (35)$$

and

$$\int_0^\infty s\left[\frac{e_{15}}{d_{11}}A_1(s, p)+A_2(s, p)\right]\sin(sx)\,ds=0 \quad (36)$$
$$0\le x<a$$

$$\int_0^\infty\left[\frac{e_{15}}{d_{11}}A_1(s, p)+A_2(s, p)\right]\cos(sx)\,ds=0 \quad (37)$$
$$a<x\le b$$

From Eqs. (36) and (37), we can find the following relation

$$A_2(s, p)=-\frac{e_{15}}{d_{11}}A_1(s, p) \quad (38)$$

and let

$$A(s, p)=c_{44}A_1(s, p) \quad (39)$$

The solution of the resulting dual integral equations (34) and (35) can be attempted by using techniques outlined in Copson (1961). That is, if we choose $A(s, p)$ given by

$$A(s, p)=\frac{\tau_0\pi a^2}{2p}\int_0^1\sqrt{\xi}\,\Omega^*(\xi, p)J_0(sa\xi)\,d\xi \quad (40)$$

where $J_0(sa\xi)$ stands for the zero order Bessel function of the first kind and $\Omega^*(\xi, p)$ is an auxiliary function.

By substituting Eq. (40) into Eqs. (34) and (35), it is easily shown that Eq. (35) is automatically satisfied, and Eq. (34) becomes the following Fredholm integral equation of the second kind:

$$\Omega^*(\xi, p)+\int_0^1\Omega^*(\eta, p)[L_1(\xi, \eta, p)-L_2(\xi, \eta, p)$$
$$+L_3(\xi, \eta)]\,d\eta=\sqrt{\xi} \quad (41)$$

with the kernels, given by

$$L_1(\xi, \eta, p) = \sqrt{\xi\eta}\int_0^\infty s[f(s/a, p)-1]J_0(s\xi)J_0(s\eta)\,ds \tag{42}$$

$$L_2(\xi, \eta, p) = (1+k^2)\sqrt{\xi\eta}\sum_{n=0}^{\infty}\pi\beta\tilde{h}^2 e^{-\Lambda/b}D(\eta, p)I_0(\Lambda\xi)I_0(\Lambda\eta) \tag{43}$$

$$L_3(\xi, \eta) = k^2\sqrt{\xi\eta}\sum_{n=0}^{\infty}\pi\beta\tilde{h}^2[\coth(\beta\tilde{h}/\tilde{b})-1]I_0(\beta\tilde{h}\xi)I_0(\beta\tilde{h}\eta) \tag{44}$$

$$f(s/a, p) = (1+k^2)\frac{\Gamma\tanh(\Gamma/\tilde{h})}{s} - k^2\tanh(s/\tilde{h}) \tag{45}$$

and

$$\tilde{h}=a/h,\ \tilde{b}=a/b,\ \tilde{b}_0=a/b_0 \tag{46a}$$

$$\Gamma=\sqrt{s^2+(pa/C_T)^2} \tag{46b}$$

$$\Lambda=\sqrt{(\beta\tilde{h})^2+(pa/C_T)^2},\quad \Lambda_e=\sqrt{(\beta\tilde{h})^2+(pa/C_{Te})^2} \tag{46c}$$

$$D(n, p)=\frac{\beta\tilde{h}[c_{44}^*(1+k^2)-Q/\Lambda]}{R(n, p)} \tag{46d}$$

$$Q=\Lambda_e\tanh\left[\Lambda_e\frac{\hat{b}-\tilde{b}_0}{\hat{b}\tilde{b}_0}\right] \tag{46e}$$

$$R(n, p)=c_{44}^*(1+k^2)\Lambda\sinh(\Lambda/\tilde{b}) + Q\cosh(\Lambda/\tilde{b}) \tag{46f}$$

$$c_{44}^*=c_{44e},\ k=\sqrt{e_{15}^2/c_{44}d_{11}} \tag{46g}$$

$I_0(\ )$ represents the modified zero order Bessel function of the first kind.

Equation (41) is the governing integral equation for the present problem, which can be solved via some existing numerical schemes.

Among the various types of electroacoustic surface waves, Bleustein-Gulyaev (B-G) waves represent peculiar solutions for the dynamic problem in piezoelectric materials, which have no counterparts in elastic media. They consist in shear horizontal electromechanical perturbations localized near the boundary surface of a piezoelectric solid and polarized perpendicularly to the sagittal plane, along a six-fold axis of material symmetry (Romeo, 2001). This shear horizontal mode surface wave velocity (Bleustein, 1968) is defined as $v_s\equiv C_T\sqrt{1-k_e^4}$ with $k_e=\sqrt{e_{15}^2/(d_{11}\mu)}$. The parameter k in Eq. (46g) is a measure of the strength of the electromechanical coupling (k_e) in the piezoelectric solid and will be referred hereafter as the electromechanical coupling coefficient (EMCC).

$$k=\frac{k_e}{\sqrt{1-k_e^2}};\quad k_e=\frac{k}{\sqrt{1+k^2}} \tag{47}$$

3. Intensity Factors

The dynamic stress and electric field can be obtained by determining the inverse of the Laplace transform of the stress and electric displacement expressions. From the point of view of fracture mechanics, however, only the singular stress near the crack tip will be derived here. The integral expression for the Laplace transform of the stress and electric displacement can be obtained by substituting Eq. (40) into Eqs. (22) and (26). The portion of $A(s, p)$ that contributes to the singular behavior is found from the integration by part of Eq. (40) in the form :

$$A(s, p)=\frac{\tau_0\pi a}{2sp}\Omega^*(1, p)J_1(as)+\cdots \tag{48}$$

where $J_1(as)$ denotes the first-order Bessel function of the first kind.

From the above result, the singular parts of the stresses and the electric displacements in the neighborhood of the crack tip can be expressed as

$$\tau_{xz}=-\frac{K^T(t)}{\sqrt{2\pi r}}\sin\left(\frac{\theta}{2}\right),\ \tau_{yz}=\frac{K^T(t)}{\sqrt{2\pi r}}\cos\left(\frac{\theta}{2}\right) \tag{49}$$

$$D_x=-\frac{K^D(t)}{\sqrt{2\pi r}}\sin\left(\frac{\theta}{2}\right),\ D_y=\frac{K^D(t)}{\sqrt{2\pi r}}\cos\left(\frac{\theta}{2}\right) \tag{50}$$

where

$$r=\sqrt{(x-a)^2+y^2},\ \theta=\tan^{-1}\left(\frac{y}{x-a}\right) \tag{51}$$

$K^T(t)$ and $K^D(t)$ are the dynamic stress intensity factor, and the dynamic electric displacement intensity factor, respectively. For a given form of the loading functions, two field intensity factors are determined as

$$K^T(t)=\lim_{x\to a^+}\sqrt{2\pi(x-a)}\,\tau_{yz}(x,\,0,\,t)=\tau_0\sqrt{\pi a}M(t) \tag{52}$$

$$K^D(t)=\lim_{x\to a^+}\sqrt{2\pi(x-a)}\,D_y(x,\,0,\,t)=\frac{e_{15}}{c_{44}}K^T(t) \tag{53}$$

where

$$M(t)=\frac{1}{2\pi i}\int_{Br}\frac{\Omega^*(1,\,p)}{p}e^{pt}dp \tag{54}$$

The function $\Omega^*(1,\,p)$ can be calculated from Eq. (41). To obtain the dynamic energy release rate, we assume that under applied loads the crack tip advances along the crack plane from $x=a$ to $x=a+\delta a$ ($\delta a\ll a$). The dynamic energy release rate during this process is identical to the mechanical strain energy release rate introduced by Park and Sun (1995a, 1995b), which is of the form:

$$G(t)=\frac{\tau_0^2\pi a}{2c_{44}}M^2(t)=\frac{[K^T(t)]^2}{2c_{44}} \tag{55}$$

It is readily seen that the dependence of the dynamic energy release rate on the dynamic stress intensity factor is the same in the form as that for purely elastic materials. Also the dynamic intensities of stress and electric displacement as well as the dynamic energy release rate are dependent upon only the resultant stress distribution generated by mechanical deformation and the electromechanical interaction (Kwon and Lee, 2001).

5. Case Studies

The solutions provided in the previous section can now be extended to several special cases; as detailed below.

(Case 1): Quasi-static solution. The corresponding static solution is obtained by applying Tauberian's final value theorem (Sneddon, 1972) as follows;

$$\Omega(\xi)+\int_0^1\Omega(\eta)\,[K_1(\xi,\,\eta)-K_2(\xi,\,\eta)]\,d\eta=\sqrt{\xi} \tag{56}$$

where

$$\lim_{p\to 0}\Omega^*(\xi,\,p)=\Omega(\xi) \tag{57}$$

$$K_1(\xi,\,\eta)=\sqrt{\xi\eta}\int_0^\infty s[f_{st}(s/a)-1]J_0(s\xi)J_0(s\eta)\,ds \tag{58}$$

$$K_2(\xi,\,\eta)=\sqrt{\xi\eta}\sum_{n=0}^{\infty}\pi\beta\tilde{h}^2e^{-\beta\tilde{h}/\tilde{b}}\left[(1+k^2)D_{st}(n)-\frac{k^2}{\sinh(\beta\tilde{h}/\tilde{b})}\right]I_0(\beta\tilde{h}\xi)\,I_0(\beta\tilde{h}\eta) \tag{59}$$

$$f_{st}(s/a)=\tanh(s/\tilde{h}) \tag{60}$$

$$D_{st}(n)=\frac{c_{44}^*(1+k^2)-\tanh\left(\beta\tilde{h}\dfrac{\tilde{b}-\tilde{b}_0}{\tilde{b}\tilde{b}_0}\right)}{c_{44}^*(1+k^2)\sinh(\beta\tilde{h}/\tilde{b})+\tanh\left(\beta\tilde{h}\dfrac{\tilde{b}-\tilde{b}_0}{\tilde{b}\tilde{b}_0}\right)\cosh(\beta\tilde{h}/\tilde{b})} \tag{61}$$

This is not in agreement with the result of Kwon and Meguid (2002) since most contents of them are derived incorrectly.

(Case 2): $\tilde{b}\to 0(b\to\infty)$. In the case, the width of the piezoelectric block is much greater than the crack length. The respective dynamic and static expressions are found to:

$$\Omega^*(\xi,\,p)+\int_0^1\Omega^*(\eta,\,p)\,L_1(\xi,\,\eta,\,p)\,d\eta=\sqrt{\xi} \tag{62}$$

$$\Omega(\xi)+\int_0^1\Omega(\eta)\,K_1(\xi,\,\eta)\,d\eta=\sqrt{\xi} \tag{63}$$

This case implies that the crack is parallel to the edges of an infinite piezoelectric strip, and Eqs. (62) and (63) are in agreement with previous results of Li and Fan (2002) and Shindo et al. (1997), respectively.

(Case 3): $\tilde{b}_0\to 0(b_0\to\infty)$. If the surrounding elastic material is an infinite strip containing a central crack parallel to the strip edges, the expressions are reduced to:

$$\Omega^*(\xi,\,p)+\int_0^1\Omega^*(\eta,\,p)\,[L_1(\xi,\,\eta,\,p)-L_4(\xi,\,\eta,\,p)+L_3(\xi,\,\eta)]\,d\eta=\sqrt{\xi} \tag{64}$$

for the dynamic impact loading with the following kernel

$$L_4(\xi,\,\eta,\,p)=(1+k^2)\sqrt{\xi\eta}\sum_{n=0}^{\infty}\pi\beta\tilde{h}^2e^{-\Lambda/b}D_1(n,\,p)\,I_0(\Lambda\xi)\,I_0(\Lambda\eta) \tag{65}$$

$$D_1(n,\ p)=\frac{\beta\tilde{h}[c_{44}^*(1+k^2)-Q_1/\Lambda]}{R_1(n,\ p)} \tag{66}$$

$$\begin{aligned}&Q_1=\Lambda_e,\ R_1(n,\ p)\\&=c_{44}^*(1+k^2)\Lambda\sinh(\Lambda/\tilde{b})+Q_1\cosh(\Lambda/\tilde{b})\end{aligned} \tag{67}$$

and

$$\begin{aligned}&\Omega(\xi)+\int_0^1\Omega(\eta)\,[K_1(\xi,\ \eta)\\&\qquad-K_3(\xi,\ \eta)]\,d\eta=\sqrt{\xi}\end{aligned} \tag{68}$$

for the corresponding static loading case with

$$\begin{aligned}K_3(\xi,\ \eta)=\sqrt{\xi\eta}\sum_{n=0}^{\infty}\pi\beta\tilde{h}^2e^{-\beta\tilde{h}/\tilde{b}}\Big[&(1+k^2)E(n)\\&-\frac{k^2}{\sinh(\beta\tilde{h}/\tilde{b})}\Big]I_0(\beta\tilde{h}\xi)\,I_0(\beta\tilde{h}\eta)\end{aligned} \tag{69}$$

$$E(n)=\frac{c_{44}^*(1+k^2)-1}{c_{44}^*(1+k^2)\sinh(\beta\tilde{h}/\tilde{b})+\cosh(\beta\tilde{h}/\tilde{b})} \tag{70}$$

(Case 4): $\tilde{h}\to 0(h\to\infty)$. Consider the case when the height of the piezoelectric composite block is much greater than the crack length. In this case, assuming $\lim_{h\to\infty}(\pi\tilde{h})=ds$; $\beta\tilde{h}=s$, the dynamic and static solutions of a piezoelectric composite strip with a central crack perpendicular to piezoelectric-elastic interface may be obtained from Eqs. (41) and (56), respectively, in the forms,

$$\begin{aligned}&\Omega^*(\xi,\ p)+\int_0^1\Omega^*(\eta,\ p)\,[L_5(\xi,\ \eta,\ p)-L_6(\xi,\ \eta,\ p)\\&\qquad+L_7(\xi,\ \eta)]\,d\eta=\sqrt{\xi}\end{aligned} \tag{71}$$

$$\begin{aligned}&L_5(\xi,\ \eta,\ p)\\&=\sqrt{\xi\eta}\int_0^\infty s[f_5(s/a,\ p)-1]J_0(s\xi)\,J_0(s\eta)\,ds\end{aligned} \tag{72}$$

$$\begin{aligned}&L_6(\xi,\ \eta,\ p)\\&=(1+k^2)\sqrt{\xi\eta}\int_0^\infty se^{-\Gamma/\tilde{b}}D_2(s,\ p)\,I_0(\Gamma\xi)\,I_0(\Gamma\eta)\,ds\end{aligned} \tag{73}$$

$$\begin{aligned}&L_7(\xi,\ \eta)\\&=k^2\sqrt{\xi\eta}\int_0^\infty[\coth(s/\tilde{b})-1]\,I_0(s\xi)\,I_0(s\eta)\,ds\end{aligned} \tag{74}$$

$$f_5(s/a,\ p)=(1+k^2)\frac{\Gamma}{s}-k^2 \tag{75}$$

$$D_2(s,\ p)=\frac{s[c_{44}^*(1+k^2)-Q_2/\Gamma]}{R_2(s,\ p)} \tag{76}$$

$$\begin{aligned}R_2(s,\ p)=&c_{44}^*(1+k^2)\,\Gamma\sinh(\Gamma/\tilde{b})\\&+Q_2\cosh(\Gamma/\tilde{b})\end{aligned} \tag{77}$$

$$Q_2=\Gamma_e\tanh\Big[\Gamma_e\frac{\tilde{b}-\tilde{b}_0}{\tilde{b}\,\tilde{b}_0}\Big] \tag{78}$$

$$\Gamma_e=\sqrt{s^2+(pa/C_{Te})^2} \tag{79}$$

and

$$\Omega(\xi)+\int_0^1\Omega(\eta)\,K_4(\xi,\ \eta)\,d\eta=\sqrt{\xi} \tag{80}$$

$$\begin{aligned}K_4(\xi,\ \eta)=\sqrt{\xi\eta}\int_0^\infty se^{-s/\tilde{b}}\Big[&\frac{k^2}{\sinh(s/\tilde{b})}\\&-(1+k^2)\,F(s)\Big]I_0(s\xi)\,I_0(s\eta)\,ds\end{aligned} \tag{81}$$

$$F(s)=\frac{c_{44}^*(1+k^2)-\tanh\Big(s\dfrac{\tilde{b}-\tilde{b}_0}{\tilde{b}\,\tilde{b}_0}\Big)}{c_{44}^*(1+k^2)\sinh(s/\tilde{b})+\tanh\Big(s\dfrac{\tilde{b}-\tilde{b}_0}{\tilde{b}\,\tilde{b}_0}\Big)\cosh(s/\tilde{b})} \tag{82}$$

(Case 5): $\tilde{h}\to 0(h\to\infty)$, $\tilde{b}_0\to 0(b_0\to\infty)$. Consider now the influence of the height and width of the composite solid. For these conditions, the expressions for the transient and static solutions are given by Eqs. (71) ~ (82):

$$\begin{aligned}&\Omega^*(\xi,\ p)+\int_0^1\Omega^*(\eta,\ p)\,[L_5(\xi,\ \eta,\ p)-L_8(\xi,\ \eta,\ p)\\&\qquad+L_7(\xi,\ \eta)]\,d\eta=\sqrt{\xi}\end{aligned} \tag{83}$$

$$\begin{aligned}&L_8(\xi,\ \eta,\ p)\\&=(1+k^2)\sqrt{\xi\eta}\int_0^\infty se^{-\Gamma/\tilde{b}}D_3(s,\ p)\,I_0(\Gamma\xi)\,I_0(\Gamma\eta)\,ds\end{aligned} \tag{84}$$

$$D_3(s,\ p)=\frac{s[c_{44}^*(1+k^2)-Q_3/\Gamma]}{R_3(s,\ p)} \tag{85}$$

$$\begin{aligned}R_3(s,\ p)=&c_{44}^*(1+k^2)\,\Gamma\sinh(\Gamma/\tilde{b})\\&+Q_3\cosh(\Gamma/\tilde{b}),\ Q_3=\Gamma_e\end{aligned} \tag{86}$$

for transient loading case, and

$$\Omega(\xi)+\int_0^1\Omega(\eta)\,K_5(\xi,\ \eta)\,d\eta=\sqrt{\xi} \tag{87}$$

$$\begin{aligned}K_5(\xi,\ \eta)=\sqrt{\xi\eta}\int_0^\infty se^{-s/\tilde{b}}\Big[&\frac{k^2}{\sinh(s/\tilde{b})}\\&-(1+k^2)\,G(s)\Big]I_0(s\xi)\,I_0(s\eta)\,ds\end{aligned} \tag{88}$$

$$G(s)=\frac{c_{44}^*(1+k^2)-1}{c_{44}^*(1+k^2)\sinh(s/\tilde{b})+\cosh(s/\tilde{b})} \tag{89}$$

for the static loading, respectively. In particular, if we impose the piezoelectric constant $e_{15}=0$ (or $k=0$), the results given in Sih and Chen (1981) will be recovered from the expression of $K_5(\xi, \eta)$. The result of Kwon and Meguid (2002) is, however, not consistent with that of Sih and Chen (1981).

(Case 6): $b=b_0$. Finally, for the case when there is only a piezoelectric block without surrounding elastic materials, the corresponding static and transient expressions are exactly reduced to those of Kwon and Lee (2000, 2001).

6. Numerical Results and Discussion

In this section, numerical results for both the static and the transient loadings are presented to show the influence of the geometry, material combinations and EMCC. Beginning from the this section, the quasi-static stress intensity factor will be expressed as SIF, the dynamic stress intensity factor will be expressed as DSIF, the quasi-static energy release rate as ERR and the dynamic energy release rate as DERR for convenience. In an attempt to obtain numerical DSIF and DERR, the obtained Fredholm integral equations are computed numerically by Gaussian quadrature integration technique. Also to carry out the numerical inversion of the Laplace transform, Miller and Guy's method (1966) is chosen because that it has been widely used in the field of fracture mechanics with a reasonable accuracy. The application of this method to Eq. (54) allows $M(t)$ to be expanded, for a suitable choice of parameters N and δ, as

$$M(T_d) \approx \sum_{n=0}^{N} q_n P_n[2\exp(-\delta T_d)-1] \tag{90}$$

where

$$T_d = C_T t/a \tag{91}$$

$$P_n(x) = \frac{(-1)^n}{2^n n!}\frac{d^n}{dx^n}[(1-x)^n(1+x)^n] \tag{92}$$

and where the coefficients q_n are evaluated iteratively from the knowledge of Ω^* at discrete points, by means of the equalities

$$\frac{\Omega^*[1, (1+n)\delta]}{1+n} = \sum_{k=1}^{n}\frac{n(n-1)\cdots[n-(k-2)][n-(k-1)]}{(n+1)(n+2)\cdots(n+k+1)} q_k, \quad n=0, 1, \cdots \tag{93}$$

The accuracy of numerical DSIF and DERR values are affected by the numerical inversion parameters such as N and δ, and Gauss Legendre and Laguerre integrating points. We use quasi-static SIF and ERR values here as a criterion to choose the value of N and δ.

Usually, the concern of practical interest in engineering applications is the case when both the surrounding elastic materials of a piezoelectric layer are thick enough ($b_0 \to \infty$) and $h \to \infty$. It corresponds to the Case 5 in section 5.

6.1 Quasi-static loading

The variation of the dimensionless SIF, $K^T/\bar{\tau}_0\sqrt{\pi a}$ ($\lim_{t\to\infty} K^T(t) = K^T$), against the dimensionless crack length, a/b, for four different ratios of $c_{44}^*(=c_{44}/c_{44e})$ is plotted in Fig. 2. When the crack is small in comparison with the layer height, $K^T/\bar{\tau}_0\sqrt{\pi a}$ remains nearly constant and not sensitive changes in c_{44}^*. As a/b increases

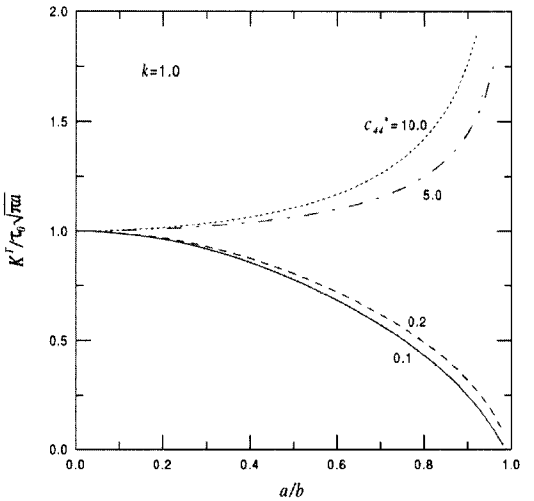

Fig. 2 Quasi-static stress intensity factor as a function $K^T/\bar{\tau}_0\sqrt{\pi a}$ of a/b

or the distance between the crack tip and interface decreases, the SIF $K^T/\tau_0\sqrt{\pi a}$ can either increase or decrease depending on c_{44}^*. Figure 3 shows that all curves do not intersect through the point $K^T/\tau_0\sqrt{\pi a}=1$ and $c_{44}^*=1$ as in a purely elastic problem (Sih and Chen, 1981) since the EMCC $k\neq 0$ in this consideration.

6.2 Transient loading

The variation of the dimensionless DERR, $\bar{G}$, versus the dimensionless time, T_d, for three different ratios of c_{44}^* is plotted in Fig. 4. Here $\bar{G}=2c_{44}G(t)/\tau_0^2\pi a$. It is seen form Fig. 4 that the curves exhibit apparent transient features similar to the ones for purely elastic media. Namely, the DERR rises quite rapidly in a small time, reaching a peak value, then drops slowly, and finally approaches to the corresponding static value. The normalized DERR $\bar{G}$ decreases when the modulus of the surrounding elastic material increases with reference to that of the

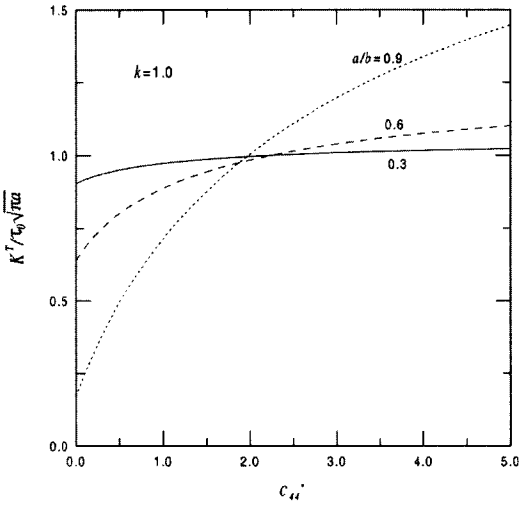

Fig. 3 Quasi-static stress intensity factor as a function $K^T/\tau_0\sqrt{\pi a}$ of c_{44}^*

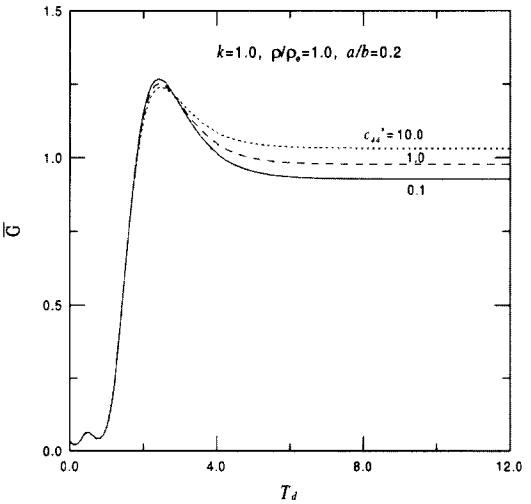

Fig. 4 Dynamic energy release rate $\bar{G}=2c_{44}G(t)/\tau_0^2\pi a$ versus T_d with the variation of c_{44}^*

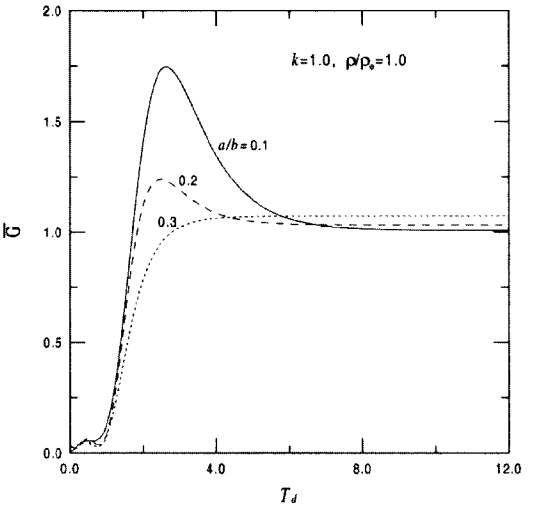

(a) $c_{44}^*=10.0$

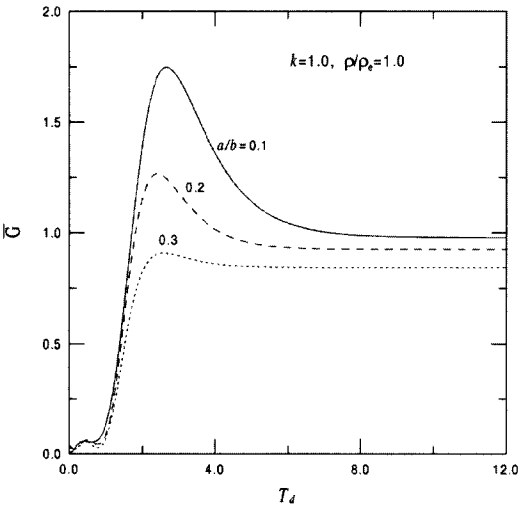

(b) $c_{44}^*=0.1$

Fig. 5 Dynamic energy release rate $\bar{G}=2c_{44}G(t)/\tau_0^2\pi a$ versus T_d with the variation of a/b

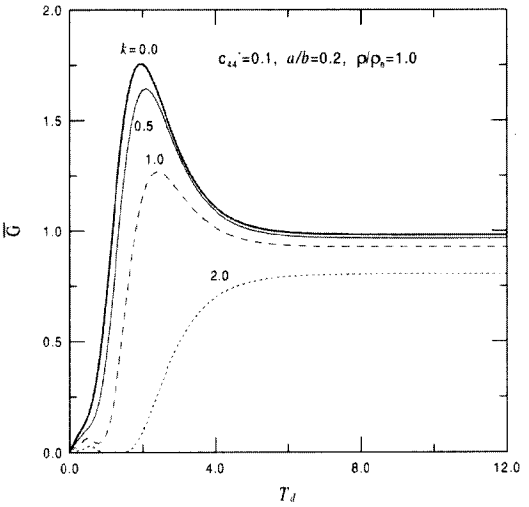

Fig. 6 Dynamic energy release rate $\bar{G}=2c_{44}G(t)/\tau_0^2\pi a$ versus T_d with the variation of EMCC k

piezoelectric layer material. The influence of a/b on $\bar{G}$ is shown in Fig. 5. The larger inertia effect on the DERR prevails at the initial stage with the decrease of the crack length, which is independent of the material combination ratio c_{44}^*. The effect of the EMCC k on the DERR is displayed in Fig. 6. It is observed that for larger EMCC, it takes longer time for DERR to reach a peak value. It is also found that the values of DERR are smaller with the increase of EMCC.

7. Conclusions

In this article, both the transient and the quasi-static responses of a cracked piezoelectric composite block with the permeable crack condition under electromechanical loads have been investigated. Using the integral transform technique, the associated mixed boundary value problem is reduced to a Fredholm integral equation of the second kind by introducing an auxiliary function. Then the electromechanical field intensity factors and the dynamic energy release rate are given explicitly in terms of the auxiliary function. The dynamic intensity factors and the dynamic energy release rate are dependent on only the resultant stress distribution generated by mechanical deformation and electromechanical interaction. It is remarked via numerical analyses that the stiffness ratio (c_{44}^*) and the electromechanical coupling coefficient (EMCC) are key parameters in the behaviors of a piezoelectric-elastic composite block.

References

Bleustein, J. L., 1968, "A New Surface Wave in Piezoelectric Materials," *Applied Physics Letters*, Vol. 13, pp. 412~413.

Chen, Z. T., 1998, "Crack Tip Field of an Infinite Piezoelectric Strip Under Anti-plane Impact," *Mechanics Research Communications*, Vol. 25, pp. 313~319.

Chen, Z. T. and Karihaloo, B. L., 1999, "Dynamic Response of a Cracked Piezoelectric Ceramic Under Arbitrary Electro-Mechanical Impact," *International Journal of Solids and Structures*, Vol. 36, pp. 5125~5133.

Chen, Z. T. and Meguid, S. A., 2000, "The Transient Response of a Piezoelectric Strip with a Vertical Crack Under Electromechanical Impact Load," *International Journal of Solids and Structures*, Vol. 37, pp. 6051~6062.

Chen, Z. T. and Yu, S. W., 1997, "Anti-plane Dynamic Fracture Mechanics in Piezoelectric Materials," *International Journal of Fracture*, Vol. 85, pp. L3~L12.

Chen, Z. T. and Yu, S. W., 1998, "Anti-plane Vibration of Cracked Piezoelectric Materials," *Mechanics Research Communications*, Vol. 25, pp. 321~327.

Copson, E. T., 1961, "On certain Dual Integral Equations," *Proceedings of the Glasgow Mathematical Association*, Vol. 5, pp. 19~24.

Crawley, E. F., 1994, "Intelligent Structures for Aerospace : a Technology Overview and Assessment," *AIAA Journal*, Vol. 25, pp. 1373~1385.

Kwon, S. M. and Lee, K. Y., 2000, "Analysis of Stress and Electric Fields in a Rectangular Piezoelectric Body with a Center Crack Under Anti-plane Shear Loading," *International Journal of Solids and Structures*, Vol. 37, pp. 4859~4869.

Kwon, S. M. and Lee, K. Y., 2001, "Transient

Response of a Rectangular Piezoelectric Medium with a Center Crack," *European Journal of Mechanics*, Vol. 20, pp. 447~468.

Kwon, S. M. and Lee, K. Y., 2004, "Dynamic Response of an Anti-plane Shear Crack in a Functionally Graded Piezoelectric Strip," *KSME International Journal*, Vol. 18, pp. 419~431.

Kwon, J. H. and Meguid, S. A., 2002, "Analysis of a Central Crack Normal to a Piezoelectric-Orthotropic Interface," *International Journal of Solids and Structures*, Vol. 39, pp. 841~860.

Li, X. F. and Fan, T. Y., 2002, "Transient Analysis of a Piezoelectric Strip with a Permeable Crack Under Anti-plane Impact Loads," *International Journal of Engineering Science*, Vol. 40, pp. 131~143.

Meguid S. A. and Wang X. D., 1998, "Dynamic Antiplane Behaviour of Interacting Cracks in a Piezoelectric Medium," *International Journal of Fracture*, Vol. 91, pp. 391~403.

Miller, M. K. and Guy, W. T., 1966, "Numerical Inversion of the Laplace Transform by Use of Jacobi Polynomials," *SIAM Journal on Numerical Analysis*, Vol. 3, pp. 624~635.

Park, S. B. and Sun, C. T., 1995a, "Effect of Electric Field on Fracture of Piezoelectric Ceramics," *International Journal of Fracture*, Vol. 70, pp. 203~216.

Park, S. B. and Sun, C. T., 1995b, "Fracture Criteria for Piezoelectric Ceramics," *Journal of the American Ceramic Society*, Vol. 78, pp. 1475~1480.

Romeo, M., 2001, "A Solution for Transient Surface Waves of the B-G Type in a Dissipative Piezoelectric Crystal," ZAMP, Vol. 52, pp. 730~748.

Shin, J. W., Kwon, S. M. and Lee, K. Y., 2001, "An Eccentric Crack in a Piezoelectric Strip Under Anti-plane Shear Impact Loading," *International Journal of Solids and Structures*, Vol. 38, pp. 1483~1494.

Shindo, Y., Tanaka, K. and Narita, F., 1997, "Singular Stress and Electric Fields of a Piezoelectric Ceramic Strip with a Finite Crack Under Longitudinal Shear," Acta Mechanica, Vol. 120, pp. 1~15.

Sih, G. C. and Chen, E. P., 1981, *Mechanics of Fracture 6 : Cracks in Composite Materials*. Edited by Sih, G., Noordhoff International Publishing, The Hague, pp. 213~218.

Sneddon, I. N., 1972, *The Use of Integral Transforms*. McGraw-Hill Book Company.